



Broadening of Convective Cells During Cold Air Outbreaks: A Numerical Study Using a Parallelized Large-Eddy Simulation Model

Siegfried Raasch, Michael Schröter

published in

NIC Symposium 2001, Proceedings,
Horst Rollnik, Dietrich Wolf (Editor),
John von Neumann Institute for Computing, Jülich,
NIC Series, Vol. 9, ISBN 3-00-009055-X, pp. 433-441, 2002.

© 2002 by John von Neumann Institute for Computing

Permission to make digital or hard copies of portions of this work for personal or classroom use is granted provided that the copies are not made or distributed for profit or commercial advantage and that copies bear this notice and the full citation on the first page. To copy otherwise requires prior specific permission by the publisher mentioned above.

<http://www.fz-juelich.de/nic-series/volume9>

Broadening of Convective Cells During Cold Air Outbreaks: A Numerical Study Using a Parallelized Large-Eddy Simulation Model

Siegfried Raasch and Michael Schröter

Institute for Meteorology and Climatology
University of Hannover, 30419 Hannover, Germany
E-mail: raasch@muk.uni-hannover.de
E-mail: schroeter@muk.uni-hannover.de

1 Introduction

The frequent occurrence of so called mesoscale cellular convection (MCC) patterns over vast regions of the oceans has been revealed by satellite imaging and its properties have been reviewed in detail by various authors¹. Areas of convective activity are usually associated with the flow of cold air over warm water such as in cold air outbreaks (CAOB). In such a case an initially cloud-free and presumably stable stratified air mass is advected from land or from an ice surface over a warmer sea surface. The heating and moistening from below causes the development of a convective boundary layer, in which a typical sequence of convection patterns can be observed: As soon as the cold air hits the warm sea, roll-like secondary flow patterns develop, appearing in satellite images as so called cloud-streets. Further downstream the roll pattern gradually changes to hexagonal cellular convection patterns, which can occur with either open or closed cells. Open cells consist of broad central areas of descending air, enclosed by relatively narrow rings of updrafts, whereas closed cells are characterized by a reversed circulation. As an example Figure 1 shows a satellite image of a CAOB situation which was observed on 10 March 1982. During this typical case of a CAOB, the whole Northern part of the Atlantic Ocean was covered by the characteristic organized convective cloud pattern.

Studying organized convection during CAOBs is of interest for at least two reasons: Firstly, the organization of convection may affect the vertical transport of heat and moisture from the water surface into the atmosphere. In CAOB regions, the sensible and latent heat flux near the surface can reach very large values (both may sum up to more than 1000 W m^{-2}). Thus CAOBs significantly contribute to the atmospheric energy balance. In weather forecast and climate models these fluxes are parameterized and therefore it is crucial to understand, how they are modified by organized convection. Secondly, there are still some open questions concerning basic features of organized convection during CAOBs. While in classical laboratory experiments of Rayleigh-Bénard convection the aspect ratio of hexagonal cells (the ratio of the cell diameter to its height) is about 3, values between 10 and 30 are typically observed during CAOBs. There are indications given by numerical simulations of CAOBs, that the release of heat due to condensation within the clouds is responsible for the cell broadening⁷. The study of the evolution of convective

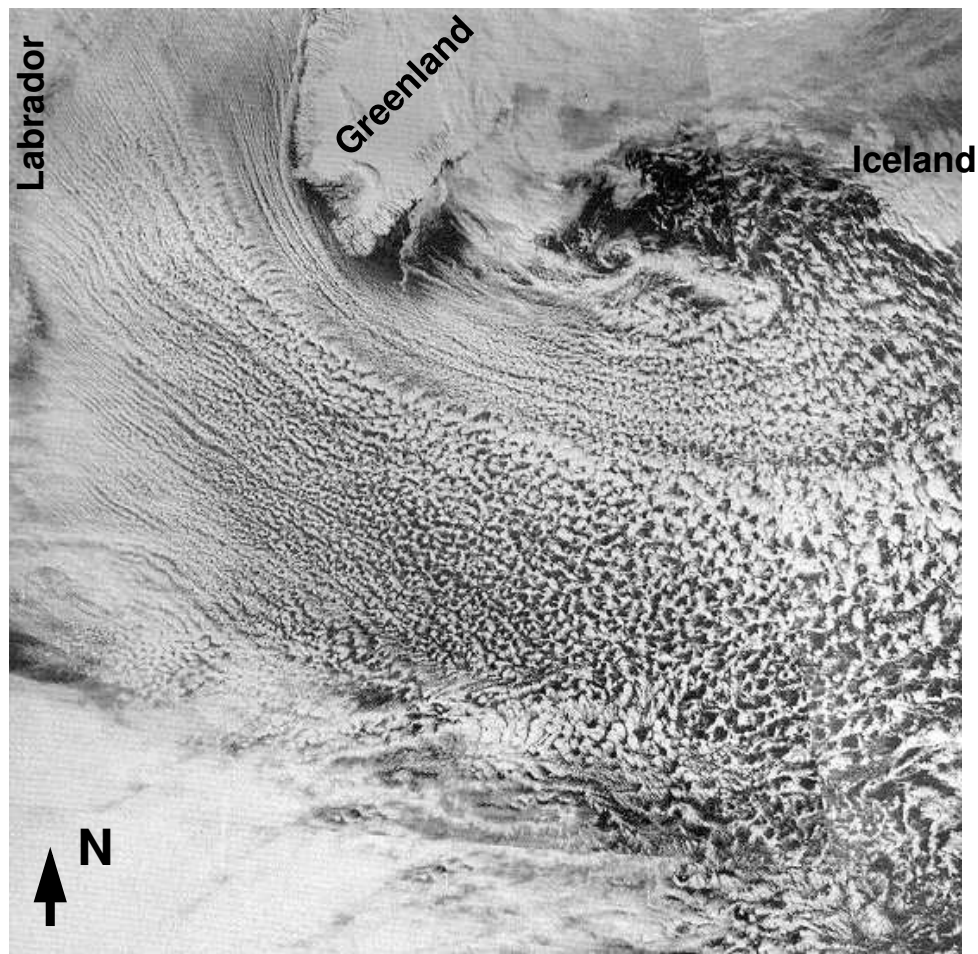


Figure 1. Cold-air outbreak situation, observed on the 10 March 1982 over the northern part of the Atlantic Ocean with the typical cloud pattern. Taken from Scorer⁹

structures of CAOBs with numerical models is only possible, when these models are able to resolve the main energy containing turbulence elements of the flow by their numerical grids. Due to insufficient computer resources, these so-called large-eddy simulations (LES) of CAOBs could not be satisfactory carried out so far, because the energy containing eddies have sizes ranging from a few hundred meters (single bubbles of warm air) up to several ten kilometers (hexagonal cells). The computational domains have to be large enough to contain the hexagonal cells and must have a spatial resolution fine enough in order to resolve also the smaller scales because possible interactions between these scales may affect the cell structure. The results of previous CAOB studies are afflicted with different uncertainties: Either the model domain was too small so that one single convection cell filled the whole model domain at the end of the simulation⁴ or a coarse resolution had to

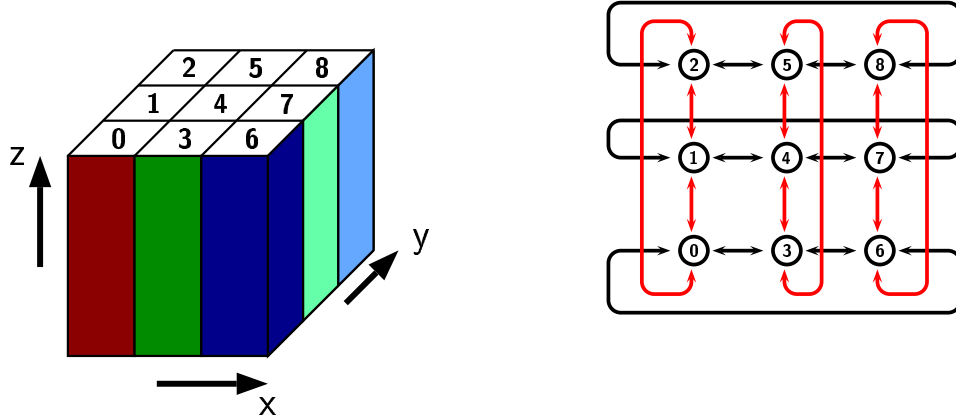


Figure 2. Principal view of the two-dimensional domain decomposition (3×3 grid) and of the virtual two-dimensional topology of processors. Subdomains of each PE are labelled with the PE number.

be used in order to be able to cover a larger area⁷.

In meteorology, LES has been used since the early 1970s as a powerful tool for studying atmospheric turbulence. First investigations relating to LES in meteorology trace back to Lilly⁶ and Deardorff³. LES models are known for their large demands on computer resources. An LES of a typical flow during a cold-air outbreak with well developed turbulence will need a computational domain of about 100 km^2 and a grid resolution of 50 to 100 m, resulting in about 10^8 grid points per variable. In case of the LES-model employed here the demand on main memory will be in the order of 30 Gbytes (provided that one word of memory is represented by 8 bytes). While in the past such simulations were impossible due to limited computer resources, the availability of parallel and massively parallel systems now offer new opportunities.

However, to get an access to the enormous computer power of parallel systems, existing models need to be extensively modified, i.e. parallelized, before they can be used efficiently on these machines. Therefore, we had to totally rewrite an existing LES code for the use on massively parallel systems. Using this new model combined with the capacity of today's massive parallel computers like the CRAY-T3E, we are able to use model domains which are large enough to guarantee that the evolving structures are not significantly restricted by the boundaries of the model domain. Additionally we can use grid spacings which are fine enough to resolve small scale convective structures like single up- and downdrafts with horizontal extensions down to 100 m, which may interact with the larger cells.

2 The Parallelized Large-Eddy Simulation Model PALM

The LES model applied here is specially designed for the use on massively parallel computers and carries the name **PALM** (**p**arallelisiertes **L**ES-**M**odell)⁸. It is based on the non-hydrostatic Boussinesq-approximated Navier-Stokes equations and contains a water cycle with cloud formation and precipitation processes. It takes into account infrared radiative cooling in cloudy conditions. The spatial derivatives are approximated by second-order

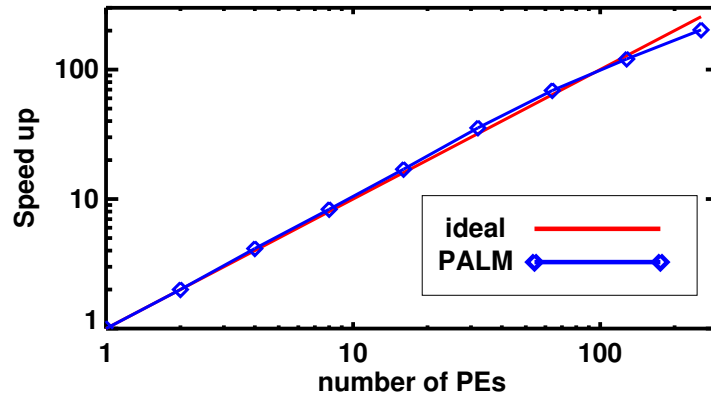


Figure 3. Speed up as a function of the number of PEs. Lines show the results for a set of test runs using $160 \times 160 \times 64$ grid points as well as the ideal case (red line)

centered finite differences. Time integration is performed by using the leap-frog scheme. Lateral boundary conditions of the model are cyclic and Monin-Obukhov similarity is assumed between the surface and the first computational grid points above.

The parallelization is achieved by horizontal two-dimensional domain decomposition as it is shown in Figure 2. The total domain is divided into subdomains, which are assigned to the processor elements (PEs) – one subdomain per each PE – and each PE solves the whole set of equations on its subdomain. Communication between the PEs is realized by the message passing interface MPI⁵. The cyclic horizontal boundary conditions are realized implicitly by creating a virtual two-dimensional topology of processors, which is shown together with the interconnecting links between the different PEs for a 3×3 grid of PEs in Figure 2.

PALM parallelizes very well and shows a good performance on distributed memory machines (CRAY-T3E) as well as on shared memory systems (SGI-Origin with 128 PEs). Figure 3 shows some results of our scalability tests on the CRAY-T3E of NIC. An almost linear speed up is achieved. Up to very large numbers of PEs (here 256 PEs) computational time is halved by doubling the number of PEs used. During all these test runs total communication time between the PEs does not exceed 8% of the total execution time (not shown). The largest run performed during our tests needs about 45 GBytes of main memory. Using 512 PEs of the CRAY-T3E at NIC and a computational grid of $1216 \times 1216 \times 160$ one timestep needs about 12 s of CPU-time on each PE for this large test run (this run seems to be a world record in resolution for LES models!⁸).

For a detailed model description and a detailed discussion of our test runs the reader is referred to Raasch and Schröter⁸ and to the world wide web^a.

^a<http://www.muk.uni-hannover.de/~raasch/PALM-1/intro.html>

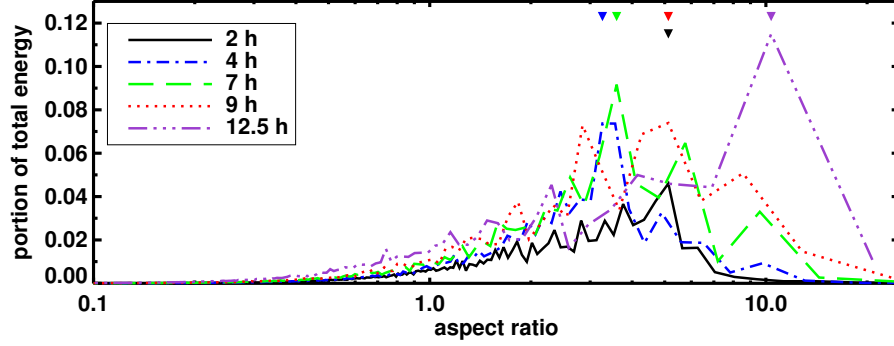


Figure 4. Vertical velocity power spectra for RUN1 resulting from two-dimensional Fourier analysis of x - y cross sections located in the middle of the developing cloud layer. An averaging of Fourier coefficients is performed in order to generate a one-dimensional presentation. Shown is the percentage of total energy as a function of the aspect ratio at different times. The aspect ratios according to dominating scales are marked by triangles.

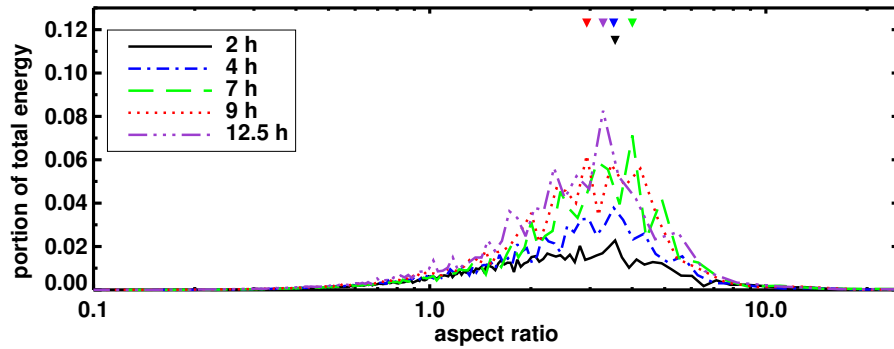


Figure 5. Vertical velocity power spectra for RUN2 resulting from two-dimensional Fourier analysis of x - y cross sections located in the middle of the boundary layer. Other features as above.

3 Broadening of Convective Cells During Cold Air Outbreaks

To study the broadening of mesoscale convection cells we refer to a CAOB situation observed during the ARKTIS 1991 experiment. On 8 March 1991 a transition of convection patterns was observed, as shown exemplarily in Figure 1. Details on the experiment are given by Brümmer². Two principal runs were performed, where we used the initialization according to the observed situation. For both runs the model domain covers an area of $70 \text{ km} \times 70 \text{ km}$ in the horizontal and 5 km in the vertical direction with a grid spacing of 100 m resulting in $700 \times 700 \times 80$ grid points. The simulations were performed on 256 PEs on the NIC CRAY-T3E covering a period of 12.5 h . Each PE required 115 CPU-h (4.8 days) in total. The first run (RUN1) includes the whole water cycle, whereas the second run (RUN2) takes the same initial parameters but the water cycle was switched off in order to study the influence of adiabatic heat sources on cell broadening.

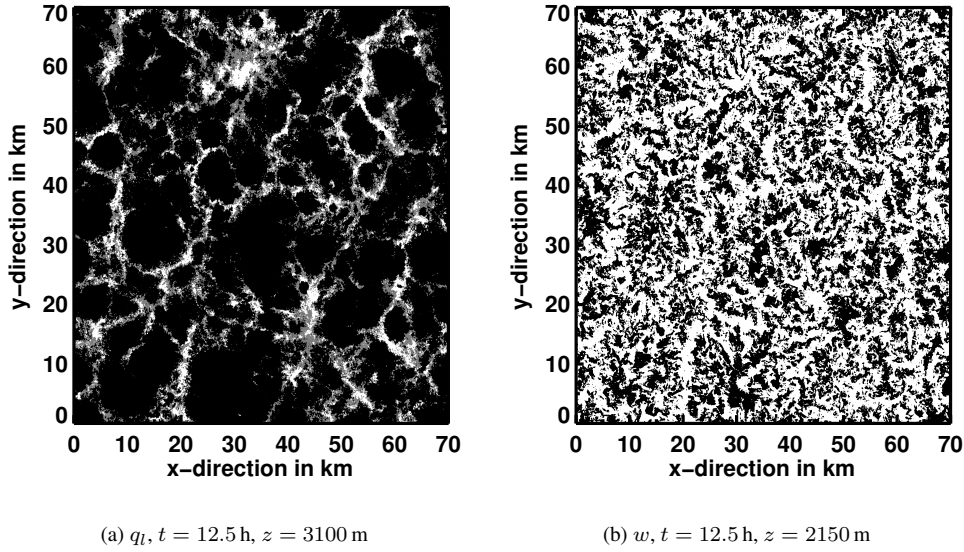


Figure 6. Contour plots of the liquid water content (left part) and of the vertical velocity (right part) in horizontal x - y - cross sections for RUN1 at $t = 12.5 \text{ h}$. Each cross section is located in the middle of the cloud layer. Left: white areas $q_l < 0.375 \text{ k kg}^{-1}$, dark areas $q_l > 0.425 \text{ k kg}^{-1}$; Right: white areas $w < 0.0$, grey and dark areas $w > 0.0$.

Figure 5 shows the power spectra of vertical velocity as a function of aspect ratio for different time levels of RUN1 and RUN2 calculated at mid boundary layer. The broadening of the dominating scales, corresponding to the mesoscale convection cells, can be seen clearly by increasing aspect ratios with increasing time. Until the end of the simulation the dominating aspect ratio increases from approximately 3.5 at 2 h and 4 h to 10 at 12.5 h. These results are in good agreement to earlier findings of other authors⁷. In contrast the power spectra of RUN2, which was performed without considering condensation and long-wave radiation processes, do not show a growing of the dominating aspect ratios. Within the whole period of the simulation the aspect ratios remain between 3 and 3.5.

Signals of the mesoscale convection cells can also be identified by visual analysis. In Figure 6 cross sections in the x - y -plane through the field of liquid water q_l and the vertical velocity field w at the end of RUN1 ($t = 12.5 \text{ h}$) in the middle of the cloud layer are shown. The centers of the cells are represented by a homogeneous distribution of relatively large values of q_l . The centers are enclosed by narrow rings represented by small values of q_l . This kind of cellular pattern is typical for so called closed convection cells. The typical diameters of the cells are in the order of 20-30 km, which is in good agreement to the observation during ARKTIS. On the first view the w -field could be characterized by spatially randomly-distributed downdrafts (light areas) and updrafts (dark areas). But on the second view cellular patterns could be identified in the w -field, due to positive correlation with the field of liquid water. In areas of small liquid water contents predominantly downdrafts can be identified. In the center of the cells the updrafts seem to be more frequent than downdrafts. Each mesoscale convection cell is an organized conglomeration of many up- and downdrafts. A phenomenon which could not be observed in earlier studies by Müller

and Chlond⁷, who used much coarser grid resolutions (up to 1600 m).

During RUN2 no formation of mesoscale convection cells could be identified. The structure of the turbulent flow and the aspect ratios observed during RUN2 agrees with the ones detected in cloudless convective boundary layers. Since in RUN2 the formation of mesoscale convection cells fails to appear, we can draw the conclusion that diabatic heat sources are responsible for the existence and for the broadening of mesoscale convection cells.

In order to point out the correlation between dynamics of the flow and its thermodynamics (temperature and liquid water content) figures 7 and 8 present cross sections in the x - z -plane through a single mesoscale convection cell. Shown are isopleths of the liquid water content and of the potential temperature for $y = 20$ km (see fig. 6). Additionally the flow dynamics are indicated by mean velocity vectors (u, w averaged over five grid points). As it should be expected from discussion above, large amounts of liquid water are in positive correlation to upwardly vertical velocities. Reaching the condensation level, water vapor condenses resulting in increasing liquid water contents (dark blue areas) and a thicker cloud layer. Due to latent heat release during the condensation process the temperature increases (red areas for $2000 \text{ m} < z < 3200 \text{ m}$). Correspondingly in areas with descending air, marked by downward pointing arrows, liquid water content and temperature decrease due to evaporation ($x \approx 15\text{-}20 \text{ km}$). Together the areas of ascending air and areas of descending air form the circulation of the mesoscale convection cells.

First attempts to answer the question about the physical processes which lead to the broadening of convective cells were made by Dörnbrack⁴ as well as by Müller and Chlond⁷. Currently, we try to verify their hypothesis using the results of our simulations. Figure 8 shows that within the cloud layer broader coherent warm and cold areas with less heterogeneity appear. These homogenous areas are invoked by stronger exchange processes which are forced by the diabatic heat sources. As a consequence the dynamic of the flow is directly affected by these broader structures.

4 Conclusions

For examinations of turbulent flows in the atmospheric boundary layer the parallelized large-eddy simulation modell **PALM** was developed for the use on massively parallel computers. Problems like the simulation of interactions between small scale and (larger scale) organized convection can be tackled now. Within these studies of organized cellular convection a simulation was performed for the first time using a turbulence resolving numerical model with a fine grid spacing combined with large horizontal extensions of the model domain. In this way we generated a dataset to study the broadening of mesoscale cellular convection resolving turbulent eddies covering a bandwidth of wavenumbers which is unmatched so far. The uncertainties of earlier investigations, using undersized model domains⁴ or using a coarse grid spacing⁷, were removed by the results of our simulations. Now it is definitely shown that diabatic heat sources like latent heat release due to condensation processes and longwave radiative cooling at the top of the cloud layer are responsible for the existence and for the broadening of mesoscale convections cells.

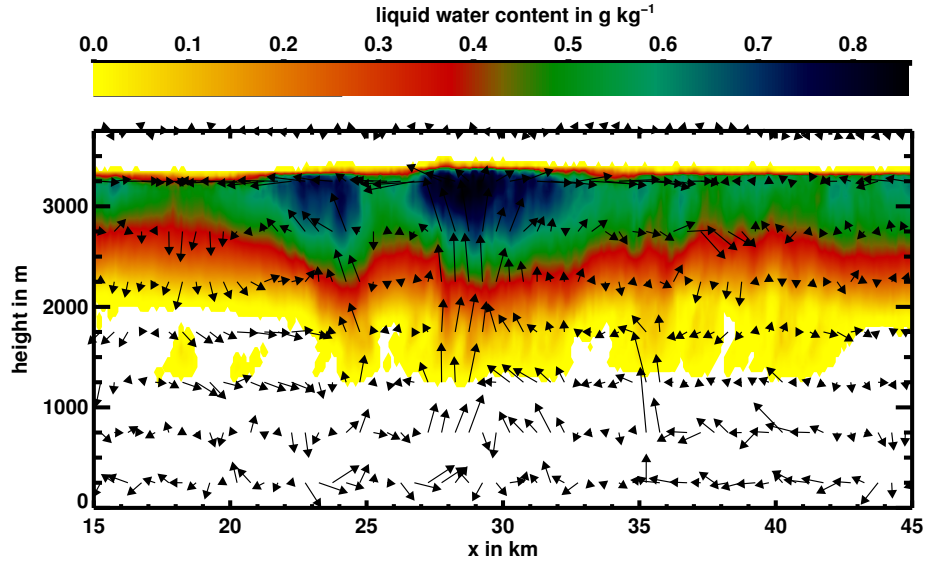


Figure 7. Contour plots of the liquid water content and a vector plot of the averaged velocity field for a vertical x - z cross section at $y = 20$ km at 12.5 h.

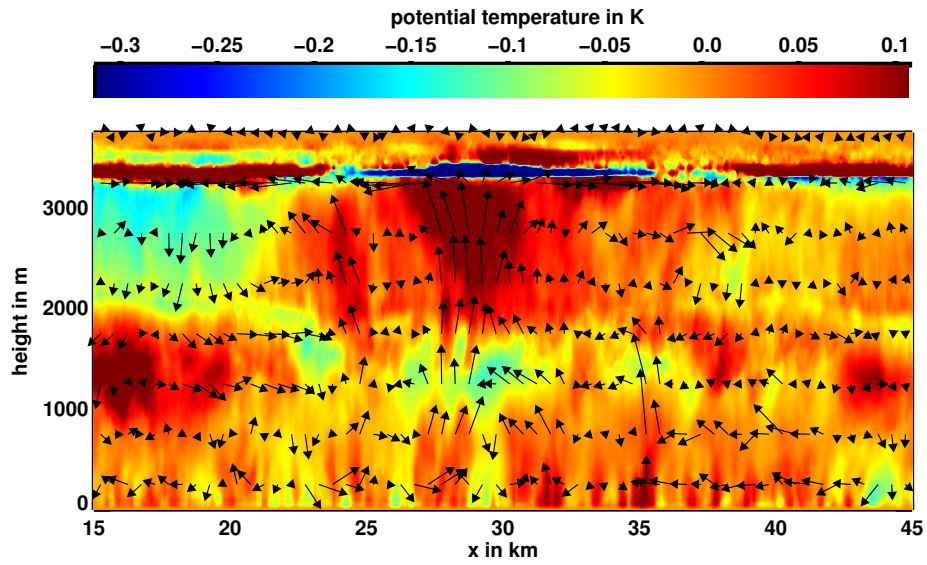


Figure 8. Contour plots of the potential temperature fluctuations and a vector plot of the averaged velocity field for a vertical x - z cross section at $y = 20$ km at 12.5 h. Temperature fluctuations are obtained by subtracting the horizontal average value calculated for each vertical grid-plane.

References

1. Agee, E. M., *Observations from space and thermal convection: A historical perspective*. — Bull. Am. Met. Soc., **65**, 938–949 (1984).
2. Brümmer, B., *ARKTIS 1991 - Report on the field phase with examples of measurements*. – Berichte aus dem Zentrum für Meeres- und Klimaforschung, Reihe A, **3**, 216 p. (1992).
3. Deardorff, J. W., *Three-dimensional numerical study of the height and mean structure of a heated planetary boundary layer*. — Boundary-Layer Meteorol., **7**, 81–106 (1980).
4. Dörnbrack, A., *Broadening of convective cells*. — Quart. J. Roy. Met. Soc., **123**, 829–847 (1997).
5. Gropp, W. E., E. Lusk and A. Skjellum, *Using MPI: Portable Parallel Programming with the Message-Passing Interface*. — MIT Press, Cambridge, 307 pp. (1994).
6. Lilly, D. K., *The presentation of small-scale turbulence in numerical simulation experiments*. – In.: Proc. IBM Scientific Computing Symp. on Environmental Sciences, Thomas J. Watson Research Center, Yorktown Heights, NY, *Three-dimensional numerical study of the height and mean structure of a heated planetary boundary layer*. 195–210 (1967).
7. Müller, G. and A. Chlond, *Three-dimensional numerical study of cell broadening during cold-air outbreaks*. — Boundary-Layer Meteorol., **81**, 289–323 (1996).
8. Raasch, S. und M. Schröter, **PALM** - *A large-eddy simulation model performing on massively parallel computers*. — Meteorol. Z., **10**, 363–372 (2001).
9. Scorer, R. S., *Cloud investigation by satellite*. – Ellis Horwood Limited, Chichester (1986).